Optimizing buried junction cubic π-SnS photocathodes

Anton Egorov, Fanxing Xi, Jonas Hepp, Lars Steinkopf, Roel van der Krol and Ibbi Ahmet

Institute for Solar Fuels

HZB Helmholtz Zentrum Berlin

Introduction:

The search for an ideal earth abundant solar absorber material for solar water splitting continues. It has been recently shown that the well known tin(II) monosulfide (SnS) semiconductor can form two polymorphs: one being the α-SnS ground state with an indirect band gap of 1.1 eV and the other being the metastable cubic π-SnS phase with a direct band gap of 1.7 eV in which both are native p-type semiconductors.[1-4] The metastable π-SnS phase has been scarcely characterised in the literature, with no known studies looking at it's properties for solar water splitting.

Here at HZB, we have been able to deposit highly crystalline thin films of both polymorphs of SnS by Aerosol Assisted Chemical Vapour Deposition (AA-CVD) with exceptional control and selectivity using zinc as a selective dopant. Our initial investigations of these samples have shown that relatively high saturated photocurrents for hydrogen evolution can be achievable, reaching ~8 mAcm^{-2} at -0.3 V_{RHE} under AM 1.5 illumination for the π-SnS phase.

These initial results present two issues:

1) The onset potential for hydrogen evolution is only +0.2 V_{RHE}, possibly due to surface recombination.
   Solution: Passivate the surface of π-SnS with a buffer layer to improve charge seperation.
2) SnS undergoe degredation under high negative bias resulting in the formation of H_2S and Sn.
   Solution: Protect the surface of the SnS with a stable protection layer.

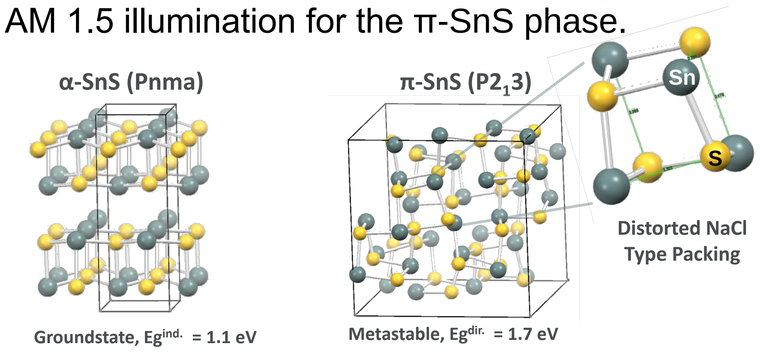

Our Investigation

In this study we fabricated a series of 2% Zn doped **π-SnS** photocathodes coated with different buffer layers consisting of **CdS**, **Zn(O,S)**, **MoS_2** or **Ag_8SnS_6**, of which the former two were coated with a 50 nm layer of TiO_2 since they were electrochemically unstable. Resultantly we were able to investigate the photo-electrochemical properties a series of π-SnS devices listed below:

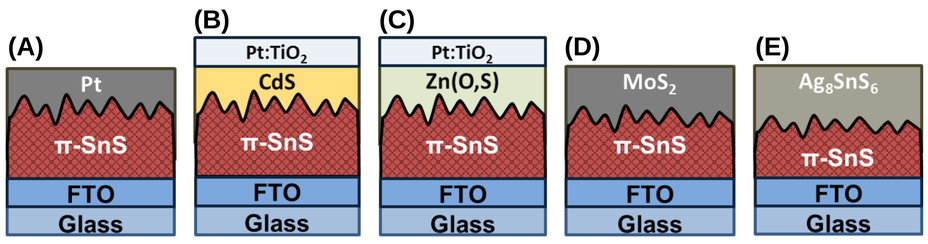

Fabrication Methods

Fig. 1: Schematic of the AA-CVD deposition process

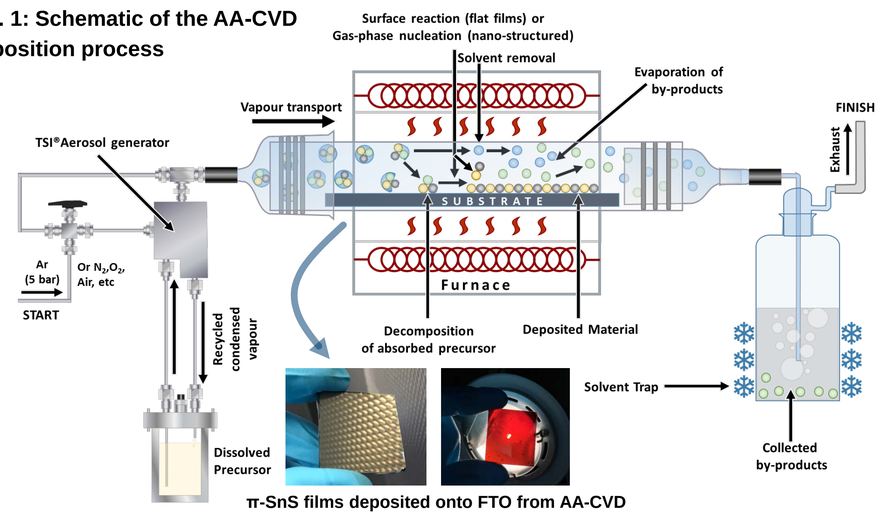

π-SnS films deposited onto FTO from AA-CVD

The π-SnS absorber layers were deposited by AA-CVD at 300-350 °C for 2 hours using a single 0.1 M solution containing $SnCl_2$, Thioacetimide and 2% $Zn(NO_3)_2$, and ethanol, ethylene glycol and acetone. ZnO, and TiO_2 layers are also deposited by AA-CVD. No post annealing was required to form a crytalline film. The CdS buffer layer was deposited by chemical bath deposition (CBD). The MoS_2 layer was deposited by magnetron sputtering and the Ag_2S layer was deposited by successive ionic layer adsorption and reaction (SILAR) methods using an ethanol solution of 0.1 M $AgNO_3$ and thioacetimide. MoS_2, Ag_2S and ZnO layers were post annealed in 5% H_2S at 350°C for 1 hour to form c-MoS_2, Ag_8SnS_6 and Zn(O,S).

CONCLUSION

- Low-cost solution fabrication methods can produce highly uniform films of π-SnS, TiO_2, ZnO, Ag_8SnS_6 and CdS, where no post annealing is required to improve the crystallinity of the films.
- The onset potential for hydrogen evolution of π-SnS photocathodes is dramatically improved when applying either a Zn(O,S) or CdS buffer layer. However, further optimisation of the photocurrent density is still required.
- Deposition of n-type MoS_2 onto π-SnS results in a ambipolar junction, which generates either a cathodic or anodic photoresponse depending on direction of illumination.
- Deposition of Ag_2S results in the formation of n-type Ag_8SnS_6 resulting in the formation of a photoanode. This further indicates that Ag can diffuse quickly into the π-SnS lattice and act as an n-type dopant.

Materials and Device Characterisation

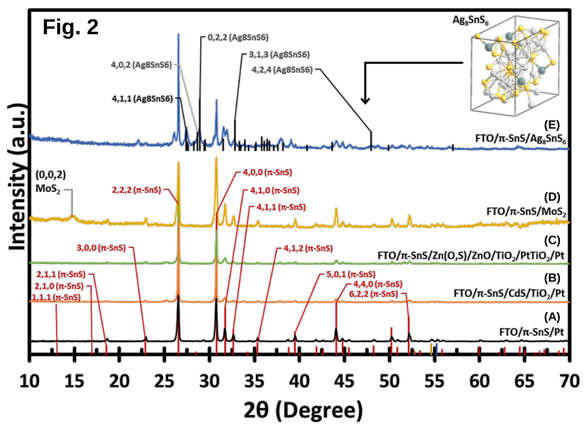

XRD analysis (**Fig. 2**) of the 5 different device configurations confirms that the π-SnS polymorph remains thermodynamically stable during all fabrication processes. For device (**D**) we identify a broad (2,0,0) peak for MoS_2, indicating that the MoS_2 has formed small crystallites, which are orientated planar to the absorber layer. For device (**E**), Ag_2S under thermal treatment reacts with SnS to form the n-type confieldite phase Ag_8SnS_6 with a band gap of ~1.30 eV.[5-7]

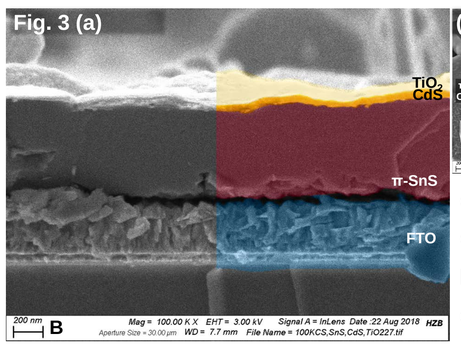

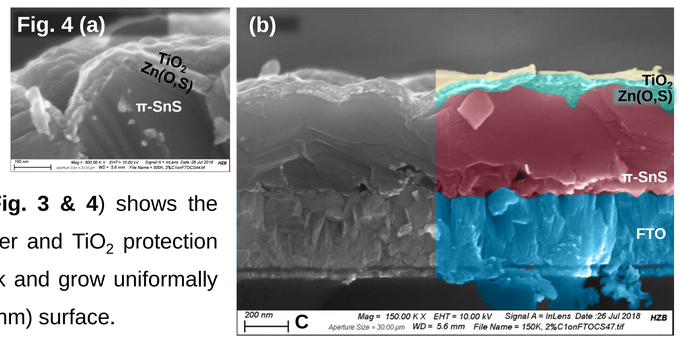

Cross-section SEM (**Fig. 3 & 4**) shows the CdS and Zn(O,S) buffer and TiO_2 protection layers are ~50nm thick and grow uniformally over the π-SnS (~800 nm) surface.

Photo-electrochemical (PEC) Performance

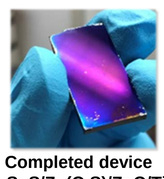

Completed device FTO/π-SnS/Zn(O,S)/ZnO/TiO_2/Pt

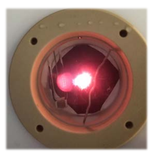

Testing the π-SnS Device in the PEC Cell

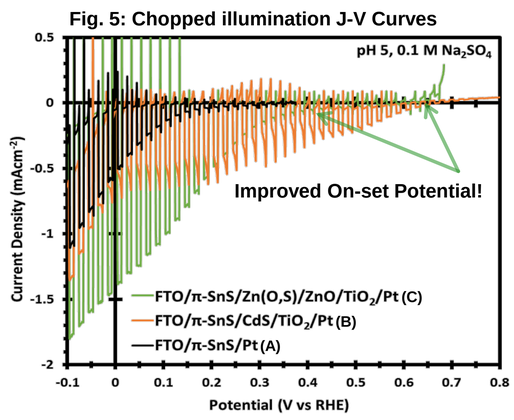

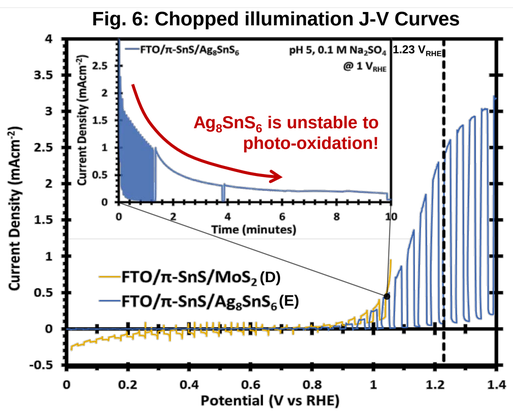

Fig.5 and **Fig.6** present the J-V curves of the different devices (**A-E**) under chopped AM 1.5 back side illumination. The photoelectrodes are in pH 5, 0.1 M Na_2SO_4 electrolyte. The electrodeposited Pt layer act as a standard electrocatalyst for hydrogen evolution. **Fig. 5** shows that by depositing a Zn(O,S) or CdS buffer layer we can increase the onset potential for hydrogen evolution, by ~200 mV using Zn(O,S) and ~600 mV using CdS. However, the photocurrent density at 0 V_{RHE} is smaller when using a CdS buffer (0.5 mAcm^{-2}) compared to using a Zn(O,S) buffer (1.5 mAcm^{-2}). **Fig.6** shows that for Device D, consisting of a π-SnS/MoS_2 junction, the cathodic photocurrent is shifted to more positive potentials (~0.6 V_{RHE}), however the photocurrent density is small. Interestingly we observed ambipolar behaviour in these devices (See **Fig.8**) such that at 0.6 V_{RHE}, illumination from the front-side (i.e. MoS_2 first) results in anodic photocurrents and illumination from the back-side (i.e. π-SnS) results in cathodic photocurrents. A similar response is observe in the open circuit voltage (OCP) measurements. Device E (Fig. **6**) is converted to a photoanode as is observed from the large anodic photocurrents and we believe this is due to the formation of n-type Ag_8SnS_6.

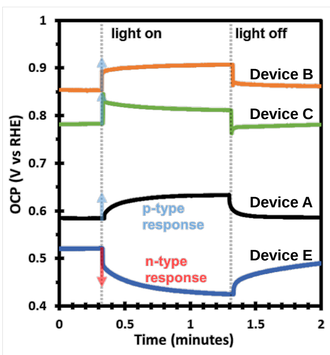

Fig. 7: Chopped illumination OCP of Devices A-C and E.

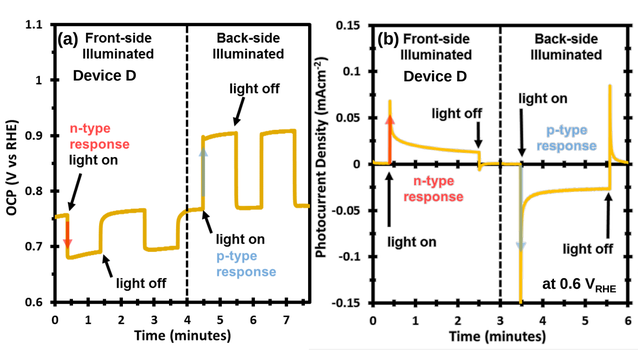

Fig 8: (a) OCP and (b)Potentiostatic Measurements of Device D with Back and Front illumination

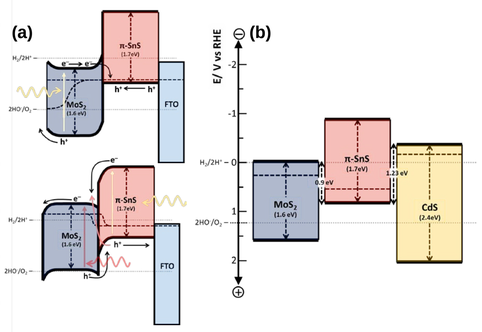

Fig 9: (a) Proposed mechanism for the high recombination and ambipolar properties of Device D. (b) Estimated band alignment diagram.

REFERENCES

(1) Abutbul, R. E. et al. *Crystal structure of a large cubic tin monosulfide polymorph: an unraveled puzzle*. CrystEngComm, **DOI:10.1039/c6ce00647g** (**2016**).
(2) Ahmet, I. Y. et al. *Polymorph-Selective Deposition of High Purity SnS Thin Films from a Single Source Precursor.* Chemistry of Materials 27, 7680-7688, **DOI:10.1021/acs.chemmater.5b03220** (**2015**).
(3) Breternitz, J. et al. *Facile Bulk Synthesis of π-Cubic SnS*. Inorganic Chemistry 56, 11455-11457, **DOI:10.1021/acs.inorgchem.7b01623** (**2017**).
(4) Sinsermsuksakul, P. et al. *Overcoming Efficiency Limitations of SnS-Based Solar Cells*. Advanced Energy Materials 4, No. 1400496, **DOI:10.1002/aenm.201400496** (**2014**).
(5) Zhu, L. *et al.* Application of facile solution-processed ternary sulfide Ag8SnS6 as light absorber in thin film solar cells. *Science China Materials*, **DOI:10.1007/s40843-018-9272-3 (2018).**
(6) Cheng, K.-W., Tsai, W.-T. & Wu, Y.-H. Photo-enhanced salt-water splitting using orthorhombic Ag8SnS6 photoelectrodes in photoelectrochemical cells. Journal of Power Sources 317, 81-92, **DOI: 10.1016/j.jpowsour.2016.03.086 (2016).**
(7) Hu, W.-Q., Shi, Y.-F. & Wu, L.-M. Synthesis and Shape Control of Ag8SnS6 Submicropyramids with High Surface Energy. Crystal Growth & Design 12, 3458-3464, **DOI: 10.1021/cg201649d (2012).**